

Control of electron–optical-phonon scattering rates in quantum box cascade lasers

D. Smirnov,^{1,*} C. Becker,² O. Drachenko,¹ V. V. Rylkov,¹ H. Page,² J. Leotin,¹ and C. Sirtori^{2,†}¹Laboratoire National des Champs Magnétiques Pulsés, 31432 Toulouse Cedex 4, France²Thales Research and Technology, 91404 Orsay Cedex, France

(Received 9 July 2002; published 20 September 2002)

Electron scattering with longitudinal-optical phonons is the main energy relaxation process between two-dimensional states in semiconductor heterostructures. This effect can be modified when the electron dispersion is broken into series of discrete states, similar to the energy spectrum of quantum boxes. This has been verified by applying a magnetic field parallel to the current of a quantum cascade laser. Light intensity as a function of the magnetic field shows pronounced oscillations, in excellent agreement with our calculations of the electron-phonon scattering rates between Landau levels.

DOI: 10.1103/PhysRevB.66.121305

PACS number(s): 63.20.Kr, 63.22.+m

When an intense magnetic field is applied perpendicularly to the *degrees* of freedom of a two-dimensional (2D) electronic system, typically a quantum well heterostructure, its energy spectrum changes completely. The continuum of states in the plane is broken by the magnetic confinement into a series of discrete levels (Landau quantization).^{1,2} The energy spectrum in this case becomes very similar to that of quantum boxes, but with highly degenerate states. This extra quantization has major consequences not only for carrier transport in the direction parallel to the plane of the quantum well,³ but also for the tunneling transport (perpendicular direction).^{4,5} The first case concerns the very active research field of the fractional quantum Hall effect⁶ and strongly correlated fermions;⁷ the second has been extensively studied in the late 1980s in double barrier resonant tunneling diodes and has given important information on the mechanisms controlling the perpendicular transport in semiconductor heterostructures.^{8,9}

In this Rapid Communication we shall show that the breaking of a 2D system into ladders of 0D states substantially modifies the lifetime of the excited energy levels. In particular, we discuss the effect of an intense magnetic field on the electron scattering rates in a quantum cascade laser.¹⁰ In this device, electrons are injected by tunneling into a two-dimensional excited state, whose lifetime is mainly controlled by the electron–longitudinal-optical (LO) phonon interaction.^{11,12} The energy of the optical phonons $\hbar\omega_{LO}$ in a crystal is practically constant,¹³ and therefore, in a system made of discrete energy states, phonon emission is either inhibited or resonantly enhanced by the presence of levels at an energy $\hbar\omega_{LO}$ below the excited state.^{14,15} Experimentally, we have observed that, for fields higher than 8 T, when the energy separation between the Landau levels exceeds the broadening of the subbands, the light intensity from the QC laser does show very pronounced oscillations as a function of the magnetic field. These oscillations are the signature of changes in the excited state lifetime, which depend on enhanced or quenched phonon emission. In the latter case, these measurements give a spectacular proof of the “optical-phonon bottleneck”^{16–19} in a semiconductor laser where the optical transitions occur between discrete energy states.^{20–22} A reduction of a factor of 2 in the threshold current between 0 and 32 T is the ultimate consequence of this bottleneck.

The device used in this study is a QC laser based on a GaAs/Al_{0.33}Ga_{0.67}As heterostructure,²³ similar to the one described in Ref. 24. The active region, shown in the inset of Fig. 1, consists of three coupled quantum wells. Three subbands ($n=1, 2$, and 3) are delocalized across this region and form the physical system that we investigated. The laser transition occurs between the $n=3$ and $n=2$ states and the lower level ($n=1$) helps a fast depopulation of the $n=2$ state by resonant optical-phonon emission. Several identical active zones are connected in series by quasiminibands that act as electron injector on one side and extractor on the other. In absence of magnetic field, the calculated lifetime of the upper laser level $n=3$ is $\tau_3 = (\tau_{31}^{-1} + \tau_{32}^{-1})^{-1} = 0.9$ ps ($\tau_{32} = 2$ ps), where τ_{31} and τ_{32} are the scattering time of the 3-1 and 3-2 intersubband transition, respectively. Under an external electric field of $F=44$ kV/cm—corresponding to the threshold voltage—we calculate a transition energy $E_{32} = 111$ meV ($\lambda = 11.2$ μm). The energy difference of the two states $n=1$ and $n=2$ is kept close to the LO phonon energy (36 meV in our material system). Figure 1 shows the spon-

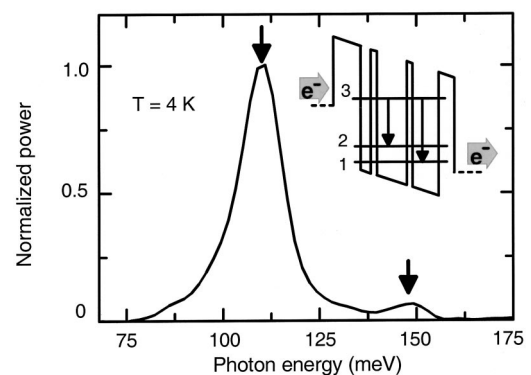


FIG. 1. Electroluminescence spectrum of the laser measured at 4 K for an injected current below threshold. The arrow at 111 meV and the arrow at 148 meV mark the position of the two peaks corresponding to the 3-2 and 3-1 transitions, respectively. Inset: Conduction-band diagram representing a portion of one period of the active region under an applied electric field of 44 kV/cm. Indicated are also the states $n=3$, $n=2$, and $n=1$. The broad gray arrows symbolize the flow of electrons that are resonantly injected into the state $n=3$ and extracted from the $n=1$ and $n=2$ states.

taneous emission spectrum of the structure measured in the pulsed mode using a Fourier transform infrared spectrometer. At 4 K, the laser transition 3-2 peaks at 111 meV ($\lambda = 11.2 \mu\text{m}$). The side peak, arising from the 3-1 transition, is blueshifted by 37 meV, in good agreement with the design of the active region. The peak corresponding to the 3-1 transition is much weaker than the 3-2 due to the specific design that concentrates most of the oscillator strength in the laser transition. The spectrum allows us to characterize the fundamental transition energies involved in the system and validates our band-structure calculations.

Forty periods of alternating active regions and injectors were grown by molecular-beam epitaxy on an n^+ GaAs substrate. The active region is sandwiched between 3.8- μm -thick low doped GaAs layers, which form the inner optical waveguide structure. Mode confinement is achieved by two highly Si doped ($4 \times 10^{18} \text{ cm}^{-3}$) plasmon layers.²⁵ The change of the refractive index, necessary for mode confinement, is achieved by a controlled variation of the doping profile of the binary GaAs claddings only.

Devices are processed into ridge lasers of 1 mm length, with facets left uncoated, mounted in the center of a coil where the magnetic field is generated by a huge pulse of current coming from the discharge of an ensemble of condensers.²⁶ The highest magnetic field reached is $B = 62 \text{ T}$, and typical experiments are performed up to $\sim 40 \text{ T}$. The current pulse peaks about 20 ms after the beginning of the discharge; at this point the magnetic field reaches its maximum value and decays with a time constant of 100 ms imposed by the impedance of the circuits. Light is detected with a boron doped silicon *blocked-impurity-band* detector with wavelength cutoff at 33 μm , mounted next to the laser facet.²⁷ Both devices are kept in liquid helium at 4 K and no collection optics is used. In this experimental configuration the detector is sensitive only to the emitted light when the *laser is above threshold* ($I_{\text{th}} = 1.7 \text{ A}$). The current is injected into the device using squared pulses, a few microseconds long and with low repetition rate, in order to avoid heating effects.

The experiment consists in monitoring the emitted light and the voltage across the device, kept under constant peak current injection, while the magnetic field is sweeping down from its maximum value. Typical results are illustrated in Fig. 2 for two different currents. In Fig. 2(a), the laser is driven below threshold at $B = 0 \text{ T}$, the light signal as a function of the magnetic field shows pronounced peaks which rise orders of magnitude above the level of noise of the detector. On the same graph, we also give an electrical characterization of the structure, with the variations of the voltage across the device as a function of the magnetic field. In accordance with the light peaks, the voltage has evident features indicating a local increase of the magnetoresistance. These are observable on top of a rising component of the voltage, which we attribute to the magnetoresistance of the miniband in the injector.²⁸ Figure 2(b) shows again the light and voltage versus magnetic field, but this time the device is above the threshold, as can be seen from the signal at low

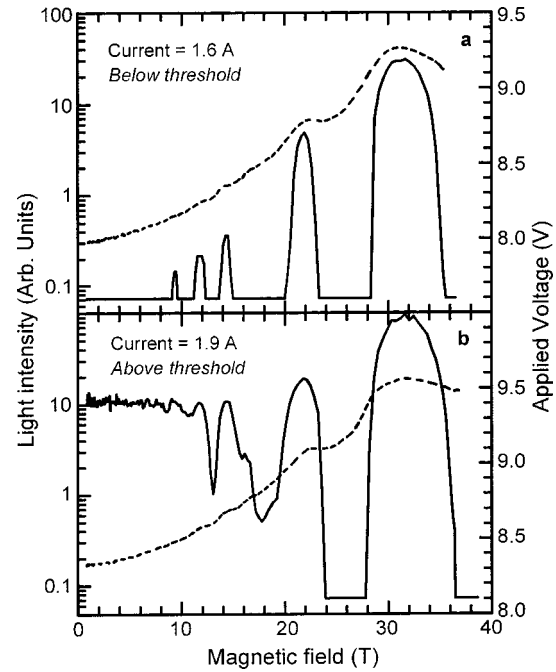


FIG. 2. Light intensity (logarithmic scale, solid lines) and voltage across the device (dashed lines) as a function of the magnetic field measured for two different currents (1.6 and 1.9 A) and at a temperature of 4 K. (a) The value of the current injected is slightly below the threshold current at zero magnetic field, 1.75 A. The background signal is fixed by the detector noise. (b) The current is higher than the threshold at $B = 0$. In both cases the light intensity is strongly modulated by the magnetic field, due to quenching or resonant enhancement of the LO-phonon emission from the $|3, 0\rangle$ state. Note that in accordance with the light maxima the voltage also increases, due to an enhancement of the lifetime.

fields. In this case the laser light is modulated above and below the value at $B = 0 \text{ T}$ and for certain fields the laser switches off.

This effect can be understood on the basis of the following physical arguments. At $B = 0 \text{ T}$, the electronic states, arising from a one-dimensional confinement, have plane-wave-like energy dispersion, in the direction parallel to the layers. The corresponding energy subbands are nearly parallel because of the small nonparabolicities.²⁹ In this case, optical-phonon emission (and/or absorption at higher temperatures) due to electrons scattering from the subband $n = 3$ towards the $n = 2$ and $n = 1$ is always allowed, because of the nearly flat dispersion of optical phonons.¹³ When an intense magnetic field is applied, the situation changes drastically: the subbands break into ladders of individual states. Neglecting the contribution due to the spin,³⁰ the energy of the electronic states evolves from $E_{n,k_{\parallel}} = E_n + \hbar^2 k_{\parallel}^2 / 2m^*(E)$ at $B = 0$, to $E_{n,l} = E_n + (l + \frac{1}{2})\hbar\omega_c$ at $B \neq 0$, where l is an integer, index of the Landau levels. In these equations, k_{\parallel} is the in-plane wave vector, $\omega_c = eB/m^*(E)$ is the cyclotron frequency, e is the electronic charge. $m^*(E)$ is the energy-dependent effective mass, imposed by the nonparabolicity.³¹ Depending on the value of the magnetic field, the configuration of the Landau levels strongly influences the emission of optical phonon from $|3, 0\rangle$, where $|n, l\rangle$ designates the Landau

level with the quantum numbers n and l . At $B=26$ T, for example, two Landau levels ($|1,3\rangle$ and $|2,2\rangle$) are separated by one LO phonon energy from the excited state of the laser transition $|3,0\rangle$. In this case, phonons can be resonantly emitted with a consequent reduction of the lifetime. This increases the threshold current and is experimentally observed in Fig. 2(b), where the laser switches off for a range of magnetic field centered at 26 T. The more common case where only one Landau level is situated 36 meV below $|3,0\rangle$ is obtained, for example, at $B=52$ T for the state $|2,1\rangle$. The situation changes completely at $B=32$ T: electrons injected into state $|3,0\rangle$ cannot lose their energy by emission of one optical phonon, since no Landau levels are present at 36 meV to preserve the energy in this process. The quenching of this scattering mechanism leads to an increase of the lifetime and thus of the electronic population on $|3,0\rangle$ (for constant injection current). This is a clear evidence of the so-called “phonon bottleneck” in a system made of highly degenerate states. The effect is mirrored in the data of Fig. 2 where the laser intensity strongly increases around 32 T and for all the other values of B corresponding to the same configuration.

We can summarize the values of the magnetic field, $B_{n,l}$, which give rise to resonant optical-phonon emission, as the solutions of the following equations: $E_{3,0} - E_{n,l}(B_{n,l}) = \hbar\omega_{LO}$ with $n=1,2$. With very good approximation this can be written as

$$\Delta E_{3-n} - \hbar\omega_{LO} = \frac{l\hbar e B_{n,l}}{m^*(E_{n,l})} \quad (n=1,2) \quad (1)$$

where ΔE_{3-n} is the energy separation between the subbands at $B=0$ T. Graphic solutions of these equations are reported in the fan chart of Fig. 3(a) up to 60 T. It must be noted that two important features have been introduced in our theoretical model for a quantitative description of this effect. First, the Landau levels are broadened by disorder and their width increases with the square root of the magnetic field;³² moreover, the curves in the fan chart are not straight lines, owing to the energy dependence of the effective mass, $m^*(E)$, due to the nonparabolicity.³¹ The light gray bands in the figure are the regions of magnetic field where the broadened Landau levels satisfy the resonant phonon-emission conditions and correspond to the series of minima of the optical power, shown in the central panel of Fig. 3. The agreement with the experiment is remarkable over the whole range of magnetic field. In the last panel of Fig. 3, we report the calculated lifetime of the $|3,0\rangle$ level as a function of the magnetic field as imposed by electron-phonon scattering. Due to the broadening and the relatively small separation of the Landau levels, the lifetime is almost constant up to 8 T. Above this value the oscillations become more pronounced and at 32 T the lifetime is approximately four times longer than at zero magnetic field. However, only a factor of 2 is measured on the current threshold which reduces to 0.9 A at 32 T. There are two main effects that can explain the smaller decrease of the laser threshold. First, electron-phonon interaction may be in competition with other scattering mechanisms that inter-

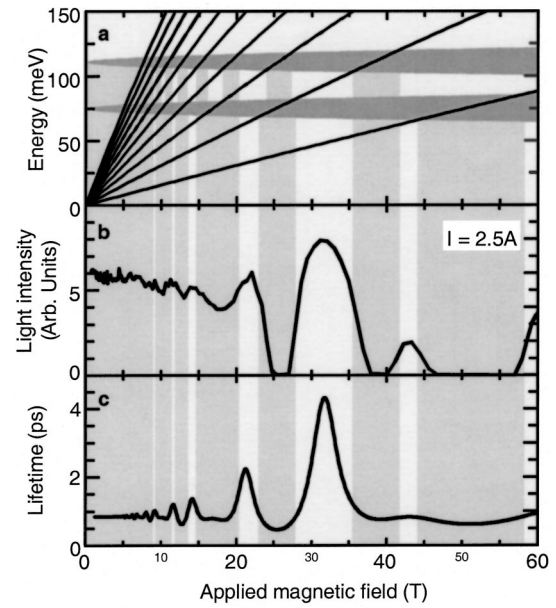


FIG. 3. (a) Calculated resonance positions as a function of the magnetic field. The dark gray areas represent the broadening of the Landau levels and are centered at $\Delta E_{3,2} - \hbar\omega_{LO} = 75$ meV and $\Delta E_{3,1} - \hbar\omega_{LO} = 111$ meV. The broadening of an individual Landau level increases with the magnetic field as σ (meV) = $\sigma_0 \sqrt{B(T)}$ with $\sigma_0 = 1$ meV/T^{1/2}. The black lines depict the equations $E = l\hbar\omega_c$ for $l=1-10$, taking into account the nonparabolicity. The overlap regions, indicated by light gray bands, correspond to the ranges of magnetic field where resonant LO-phonon emission occurs. (b) Measured light intensity as a function of the magnetic field (up to 60 T) with an injected current of 2.5 A (above threshold). (c) Calculated lifetime of the state $n=3$ as a function of the magnetic field.

vene when the electron-phonon scattering is quenched; second, the tunneling time out of the $|2,0\rangle$ and $|1,0\rangle$ levels into the injector can increase with the magnetic field, thus reducing population inversion. The absolute minimum of the lifetime occurs at 26 T, in correspondence with the special double resonant condition, which has been described before.

In our calculations of the lifetime, we start by using the Fermi golden rule to derive scattering rates of an electron initially in state $|3,0\rangle$, which relaxes into lower Landau levels $|n,l\rangle$ ($n=1,2$), situated one LO-phonon energy below. This configuration corresponds to a magnetic field $B_{n,l}$, given by Eq. (1). At this magnetic field, the scattering rates read

$$\tau_{3,0}^{-1}(n,l) = \frac{2\pi}{\hbar} \int dE \int \frac{d^3\mathbf{q}}{(2\pi)^3} |\langle 3,0 | H_{e-ph}(\mathbf{q}) | n,l \rangle|^2 \times \delta(E - \hbar\omega_{LO}) f_{3,0;n,l}(E, B_{n,l}), \quad (2)$$

where, \mathbf{q} is the phonon wave vector and $H_{e-ph}(\mathbf{q})$ is the electron-phonon Hamiltonian in the bulk phonon approximation. The Dirac function expresses the energy conservation and $f_{3,0;n,l}(E, B_{n,l})$ is the joint density of states between $|3,0\rangle$ and $|n,l\rangle$, which are considered as broadened states with a Gaussian-like energy distribution. As it has been already mentioned, the width of the Gaussian depends on B as

$\sigma(B) = \sigma_0 \sqrt{B}$, with $\sigma_0 = 1 \text{ meV/T}^{1/2}$. The value of σ_0 has been adjusted so as to reproduce the main features observed experimentally and is in exact agreement with what has been already reported in the literature.³³

To obtain the total value of the scattering rates at all magnetic fields, we sum the contributions arising from Landau levels with different n and l , weighted by the normalized factor $P_{3,0;n,l} = f_{3,0;n,l}(\hbar\omega_{LO}, B) / f_{3,0;n,l}(\hbar\omega_{LO}, B_{n,l})$,

$$\tau_{3,0}^{-1}(B) = \sum_{n,l} \tau_{3,0}^{-1}(n,l) P_{3,0;n,l}(B). \quad (3)$$

Our calculations are in very good agreement with the experiments using GaAs bulklike phonons. This is expected considering that the high gap material in the heterostructure is an alloy of AlGaAs with 33% Al content and therefore the variation of the dielectric constant between the two materials is weak and not sufficient to produce confined phonon structures. The situation can be completely different in the heterostructure made of AlAs/GaAs, where these measurements can give important information on the energies of the different phonon modes and their respective weight on the scatter-

ing rates with the electrons. More generally, we believe that this technique can be used for phonon spectroscopy in compound semiconductor heterostructures. Our calculations suggest that, using a simplified QC active region made of a single quantum well, distinct modulations of the intersubband light emission can be detected in the 5–15 T range. These magnetic fields are attainable in continuous wave by standard superconductor coils, which make the experiment much simpler.

In conclusion, we have shown that the electron-optical phonon interaction, the dominant energy relaxation process for 2D energy levels, can be strongly modified by reducing the dimensionality of the system. This has been demonstrated by applying an intense magnetic field on a quantum cascade laser, which changes its continuum energy spectrum into a series of discrete states, as in quantum boxes. The intensity of the light and the threshold of the device depend on the field and are in excellent agreement with the phonon resonances (antiresonances) predicted by the theory. This experiment opens more avenues for the research on quantum cascade lasers based on low (1D, 0D)-dimensional structures and suggests a method for the spectroscopy of (confined)-phonon modes.

*Permanent address: Ioffe Physico-Technical Institute, 194021 St. Petersburg, Russia.

†Corresponding author. Email address: carlo.sirtori@thalesgroup.com

¹L. D. Landau and E. M. Lifshitz, *Quantum Mechanics: Non Relativistic Theory* (Pergamon, London, 1959).

²T. Ando, A. B. Fowler, and F. Stern, *Rev. Mod. Phys.* **54**, 437 (1982).

³K. von Klitzing, G. Dorda, and M. Pepper, *Phys. Rev. Lett.* **45**, 494 (1980).

⁴E. E. Mendez, L. Esaki, and W. I. Wang, *Phys. Rev. B* **33**, 2893 (1986).

⁵M. L. Leadbeater *et al.*, *Phys. Rev. B* **39**, 3438 (1989).

⁶D. C. Tsui, H. L. Stormer, and A. C. Gossard, *Phys. Rev. Lett.* **48**, 1559 (1982).

⁷R. B. Laughlin, *Rev. Mod. Phys.* **71**, 863 (1999).

⁸C. H. Yang, M. J. Yang, and Y. C. Kao, *Phys. Rev. B* **40**, 6272 (1989).

⁹G. S. Boebinger *et al.*, *Phys. Rev. Lett.* **65**, 235 (1990).

¹⁰J. Faist *et al.*, *Science* **264**, 553 (1994).

¹¹P. J. Price, *Ann. Phys. (San Diego)* **133**, 217 (1981).

¹²R. Ferreira and G. Bastard, *Phys. Rev. B* **40**, 1074 (1989).

¹³P. Y. Yu and M. Cardona, *Fundamentals of Semiconductors, Physics and Materials Properties*, (Springer-Verlag, Berlin, Berlin, 1996).

¹⁴P. D. Buckle *et al.*, *Phys. Rev. B* **53**, 13 651 (1996).

¹⁵D. Bertram *et al.*, *Phys. Rev. B* **56**, R7084 (1997).

¹⁶U. Bockelmann and G. Bastard, *Phys. Rev. B* **42**, 8947 (1990).

¹⁷H. Benisty, C. M. Sotomator-Torrès, and C. Weisbuch, *Phys. Rev. B* **44**, 10 945 (1991).

¹⁸B. N. Murdin *et al.*, *Phys. Rev. B* **59**, 7817 (1999).

¹⁹J. Urayama *et al.*, *Phys. Rev. Lett.* **86**, 4930 (2001).

²⁰B. Lax, in *Proceedings of the International Symposium on Quantum Electronics*, edited by C. H. Townes (Columbia Univ. Press, New York, 1960).

²¹H. Aoki, *Appl. Phys. Lett.* **48**, 559 (1986).

²²A. Kastalsky and A. L. Efros, *J. Appl. Phys.* **69**, 841 (1991).

²³C. Sirtori *et al.*, *Appl. Phys. Lett.* **73**, 3486 (1998).

²⁴P. Kruck *et al.*, *Appl. Phys. Lett.* **76**, 3340 (2000).

²⁵C. Sirtori *et al.*, *Appl. Phys. Lett.* **75**, 3911 (1999).

²⁶O. Portugall *et al.*, *Physica B* **294–295**, 579 (2001).

²⁷S. Pasquier *et al.*, *J. Appl. Phys.* **83**, 4222 (1998).

²⁸A detailed analysis of the electrical characteristics will be given in another paper [D. Smirnov *et al.* (unpublished)].

²⁹R. P. Leavitt, *Phys. Rev. B* **44**, 11 270 (1991).

³⁰The spin splitting in GaAs/Al_xGa_{1-x}As heterostructure is very small and does not exceed 2 meV even at 60 T. It is therefore always contained within the broadening of the Landau levels. See, e.g., M. J. Snelling *et al.*, *Phys. Rev. B* **44**, 11 345 (1991).

³¹C. Sirtori *et al.*, *Phys. Rev. B* **50**, 8663 (1994).

³²T. Ando and Y. Uemura, *J. Phys. Soc. Jpn.* **36**, 959 (1974).

³³J. P. Eisenstein *et al.*, *Phys. Rev. Lett.* **55**, 875 (1985).